Available online at www.sciencedirect.com
SCIENCE DIRECT®
Journal of Nuclear Materials 335 (2004) 39–47
journal of nuclear materials
www.elsevier.com/locate/jnucmat

Post-irradiation examination of uranium–7 wt% molybdenum atomized dispersion fuel

A. Leenaers [a,*], S. Van den Berghe [a], E. Koonen [a], C. Jarousse [b], F. Huet [c], M. Trotabas [d], M. Boyard [e], S. Guillot [e], L. Sannen [a], M. Verwerft [a]

[a] SCK • CEN, Reactor Materials Research, Boeretang 200, B-2400 Mol, Belgium
[b] Compagnie pour l'Etude et la Réalisation de Combustibles Atomiques CERCA, ZI Les Bérauds, 26104 Romans, France
[c] Commissariat à l'énergie atomique (CEA) Cadarache, DENCAD-DEC-SESC, 13108 Saint-Paul-lez-Durance cedex, France
[d] SRMJ, 12/4 rue de St. Nom, 78620 l'Etang la ville, France
[e] TECHNICATOME, BP 34000, 13791 Aix-en-Provence cedex 3, France

Received 6 April 2004

Abstract

Two low-enriched uranium fuel plates consisting of U–7wt%Mo atomized powder dispersed in an aluminum matrix, have been irradiated in the FUTURE irradiation rig of the BR2 reactor at SCK • CEN. The plates were submitted to a heat flux of maximum 353 W/cm^2 while the surface cladding temperature is kept below 130 °C. After 40 full power days, visual examination and profilometry of the fuel plates revealed an increase of the plate thickness. In view of this observation, the irradiation campaign was prematurely stopped and the fuel plates were retrieved from the reactor, having at their end-of-life a maximum burn-up of 32.8% ^{235}U (6.5% FIMA). The microstructure of one of the fuel plates has been characterized in an extensive post-irradiation campaign. The U(Mo) fuel particles have been found to interact with the Al matrix, resulting in an interaction layer which can be identified as (U,Mo)Al_3 and (U,Mo)Al_4. Based on the composition of the interaction layer it is shown that the observed physical parameters like thickness of the interaction layer between the Al matrix and the U(Mo) fuel particles compare well to the values calculated by the MAIA code, an U(Mo) behavior modeling code developed by the Commissariat à l'énergie atomique (CEA).

1. Introduction

The high-temperature isotropic uranium γ-phase behaves rather stable under irradiation compared to its room temperature α-phase structure. A transformation of γ to α (through the β phase) cannot be suppressed by quenching the high-temperature γ phase. However, the temperature range over which the α, β, and γ phase are stable can be altered by alloying the material [1,2].

Molybdenum exhibits a high degree of solid solubility in γ-uranium. If cooled slowly or if the alloy contains less than 7 at.% Mo [1], the equilibrium state of U(Mo) alloys below 560 °C is a mixture of α-U and a γ′-phase (U_2Mo). By quenching the U(Mo) alloy from the γ-phase, a metastable γ-state will be retained at room temperature. U(Mo) alloys have been considered as one of the most promising uranium alloys to be used

* Corresponding author. Tel.: +32 14 333044; fax: +32 14 321216.
E-mail address: aleenaer@sckcen.be (A. Leenaers).

0022-3115/$ - see front matter © 2004 Elsevier B.V. All rights reserved.
doi:10.1016/j.jnucmat.2004.07.004

as dispersion fuel due to the good irradiation performance of its cubic γ-phase.

The French program for U(Mo) fuel qualification, launched in 1999, is a close collaboration between Compagnie pour l'Étude et la Réalisation de Combustibles Atomiques (CERCA), the Commissariat à l'énergie atomique (CEA), FRAMATOME Advanced Nuclear Power (ANP), TECHNICATOME and the Compagnie Générale des Matières Nucléaires (COGEMA). To contribute to the development of U(Mo) dispersion fuel, the French group has decided to irradiate full-sized experimental plates with low enriched uranium (^{235}U = 19.8%) and high uranium loading up to 8.5 g/cm^3. Fuel plates consisting of ground or atomized U(Mo) powder dispersed in an aluminum matrix and surrounded by an aluminum alloy cladding have been produced by CERCA. The U–7wt%Mo ground powder fuel plates were successfully irradiated in the IRIS device of the OSIRIS I reactor [3,4]. The maximum surface power of fuel plates during the IRIS experiment has been 136 W/cm^2, while the cladding temperature was kept below 75 °C. After 241 full power days (FPD), the fuel plates had a peak burn-up of 67.5% ^{235}U (13.3% FIMA) and demonstrated a swelling lower than 6%.

The fuel plates containing U–7wt%Mo atomized powder have been irradiated in the FUTURE irradiation rig of the BR2 reactor at SCK • CEN. The objective of the program was to test the behavior of this type of fuel while irradiating with a surface heat flux up to 353 W/cm^2 and a maximum fuel cladding temperature of 130 °C during operation. After the second irradiation cycle, visual examination and profilometry of the atomized U(Mo) fuel plates showed a local increase of 13% in plate thickness in the axial hot plane and the plates were retrieved from the reactor. After 40 FPD's, the fuel plates had a maximum burn-up of approximately 33% ^{235}U (6.5% FIMA or 1.41×10^{21} fissions/cm^3 meat).

A sample of the most deformed area was taken and submitted to a post-irradiation campaign. The microstructure of the U(Mo) fuel was analyzed by optical microscopy (OM), scanning electron microscopy (SEM) and electronprobe microanalysis (EPMA). During the PIE special attention was given to the composition of the interaction layer which is formed due to reaction between the Al matrix and the U(Mo) fuel particles.

2. Experimental procedures

2.1. Production of U–7wt%Mo dispersion fuel

The fuel plates were manufactured by CERCA, using low-enriched U–7wt%Mo (measured 7.3 wt% Mo) atomized powder supplied by the Korea Atomic Energy Research Institute (KAERI). The atomized powder was heat-treated for several hours to ensure a complete transformation to the γ-phase and quenched. The fuel powder, containing particles of less than 125 μm was mixed with aluminum powder (A5) according to a U(Mo)/Al mass ratio of 7.32. The mixed powder was then successively compacted, placed into the aluminum cladding frames and hot rolled. The cladding consists of AG3-NET, an aluminum magnesium alloy (2.8 wt% Mg) which corresponds to a nuclear grade Al 5754 alloy. The final fuel loading amounts to 8.47 U g/cm^3 and a porosity of 1.1% was measured.

It should be noted that the U–7wt%Mo atomized fuel plates were not incorporated as curved segments in a BR2 fuel element, but have been irradiated in a flat plate configuration in the FUTURE rig.

2.2. Sample preparation and experimental techniques

After the two irradiation cycles, a sample was cut from the most deformed area located at the highest flux position, which is characterized by a maximum count rate in the axial and transverse direction of the gross gamma spectrum. For reason of comparison, a sample of a sibling unirradiated fuel plate was taken. The samples were embedded in an epoxy resin in such a way that the complete section of the fuel plate (meat and cladding) can be observed. The samples were polished with SiC paper of successively finer grain size, finishing on cloth with diamond paste of 3 and 1 μm.

Optical microscopy was performed on a Reichert Telatom 3 remote controlled and shielded optical microscope. Observations on the samples were made in as-polished and etched conditions. The etchant, consisting of 38 ml HNO_3 (65%) 1 ml HF (38%) and 100 ml H_2O [5] was used to reveal the cellular structure of the U(Mo) particles. The sample was immersed in the solution for up to a few minutes.

The electronprobe microanalysis (EPMA) was performed on a shielded CAMEBAX-R Microbeam, upgraded with digital image and X-ray acquisition programs (SAMx Suite). X-ray mappings were recorded to obtain the distribution of several elements (Al, Mo, U, Xe and Nd), and the semi-quantitative elemental composition at discrete points on the fuel plates was measured by wavelength dispersive X-ray analysis (WDX). Prior to each measurement, calibration was performed using the appropriate standards (Table 1). For scanning electron microscopy (SEM) a shielded JEOL scanning electron microscope type 6310 was used in secondary electron image mode.

X-ray diffraction (XRD) data of the unirradiated sample were recorded on a Philips X'Pert θ–θ diffractometer equipped with a Cu tube (CuK$\alpha_{1,2}$ = 0.1541 nm), configured in the standard Bragg-Brentano geometry. Scans of the diffraction peaks in the 30–80° 2θ range were recorded with the X'Celerator, an X-ray area detec-

Table 1
Crystals used for X-ray mapping and quantitative EPMA analysis

Element	X-ray line	Wavelength (pm)	Crystal	Standard
Al	Kβ	794.0	TAP	Al_2O_3
Mo	Lα	540.7	PET	Mo (pure)
Xe	Lα	301.7	PET	Interpolation
Nd	Lα	237.1	LIF	NdF_3
U	Mα	391.0	PET	U (pure)

Prior to the quantification of the elements, calibration is performed using the appropriate standards. The correction factor for Xe is obtained by interpolation of the values acquired from Sb, Te, I and Cs standards.

tor based on real time multiple strip (RTMS) technology.

3. Microstructure of U–7wt%Mo fuel plates

3.1. Observations on the unirradiated U(Mo) fuel plate

The phases present in the U(Mo) powder of the sibling sample are measured by X-ray diffraction. To obtain a larger analysis surface, the cladding at one side of the unirradiated sample is removed by polishing until the meat becomes visible. The measured X-ray diffraction pattern (Fig. 1) shows that the powder, after fabrication but prior to irradiation, contains a significant amount of orthorhombic α-U in addition to γ-U. Diffraction peaks due to the Al of the cladding and matrix are also present.

It can be seen from the detailed optical microscopy image (Fig. 2(a)) of a U(Mo) fuel particle of the unirradiated sample in as-polished condition, that the spherical U(Mo) particles consist of smaller grains and as such give a cellular aspect to the structure of the fuel particles. This cellular structure is a result of rapid solidification during the atomization process [6]. Previous studies have shown that the structure consists of a Mo-enriched cell interior and a Mo-depleted cell boundary, with a compositional difference of approximately 2 wt% [6–8].

It was observed in the current study that the cells at the edge of the particle appear to be smaller and more elongated than the cells in the center of the fuel particle. There is no indication of the formation of an interaction layer between the U(Mo) fuel particle and the Al matrix after fabrication, prior to the irradiation (Fig. 2(a)).

3.2. Post-irradiation observations

After irradiation, the cellular structure in the fuel particles can only be observed after polishing and etching of the sample (Fig. 2(b)). In the same micrograph, it is seen that an interaction between the Al matrix and the U(Mo) fuel particle has occurred, resulting in a U–Mo–Al layer surrounding the fuel particle. The composition of this layer is discussed in the next section. Small voids are observed at the interface of the U–Mo–Al interaction layer and the Al matrix.

A composition of optical micrographs (Fig. 3(a)) covering the complete width of the sample reveals that the deformed area is located near the center of the image. At that location (Fig. 3(a1)), large porosities can be observed which are in part due to pull-out during

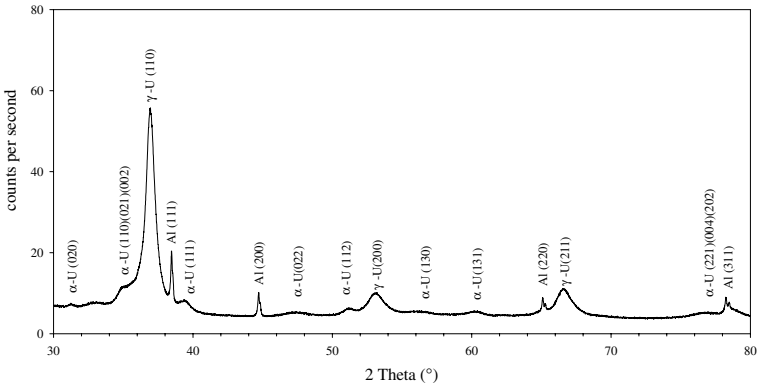

Fig. 1. X-ray diffraction pattern of the unirradiated sample shows that the U(Mo) powder contains an amount of α-uranium next to the desired γ-uranium. The indexed Al peaks originate from the fuel matrix and/or cladding.

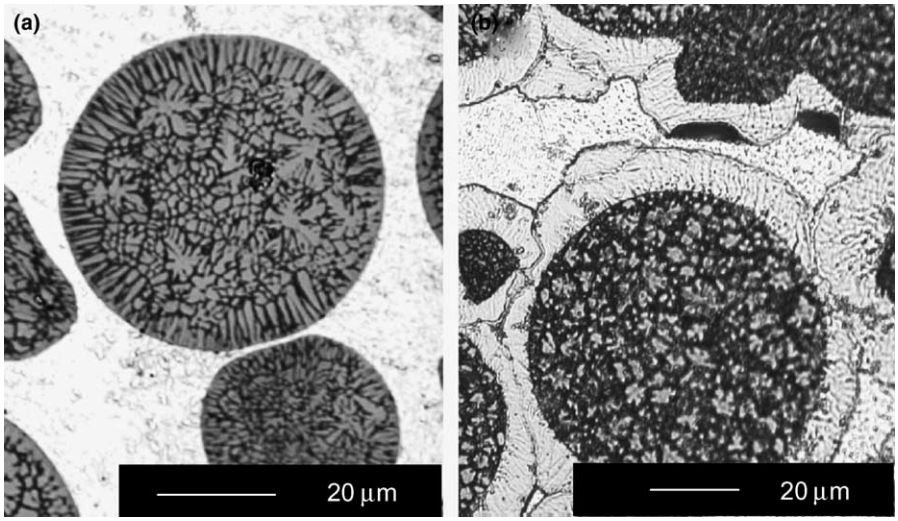

Fig. 2. The cellular structure of the fuel particles in the unirradiated U–7wt%Mo fuel plate (a) and in the irradiated fuel plate (b), is due to rapid solidification during atomization. Opposed to the unirradiated fuel particle, the formation of an interaction layer, surrounding the fuel particle, has occurred during irradiation.

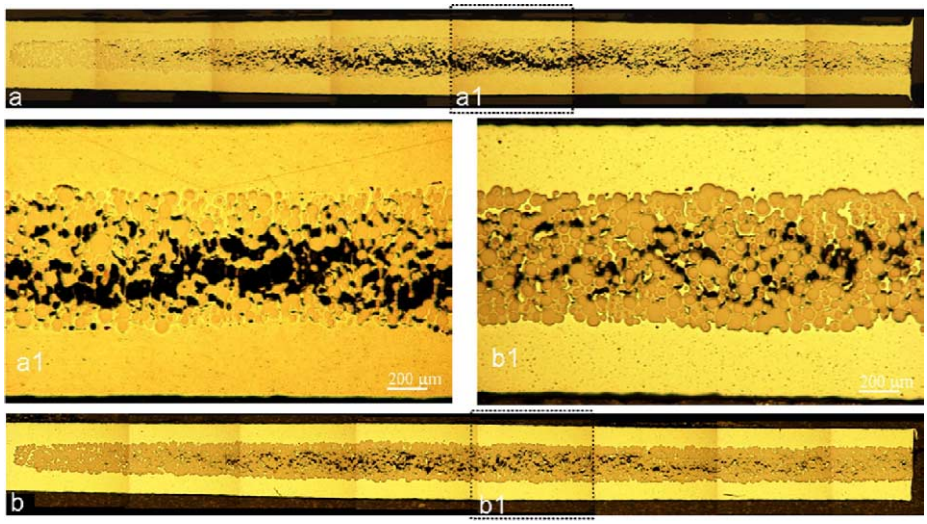

Fig. 3. A composition of optical micrographs (a) of the irradiated sample reveals the increase in fuel meat thickness. The large porosities in the central area of the image (a1) are due to sample preparation. After impregnating and repolishing of the sample, most of these large porosities are no longer observed (b, b1).

sample preparation. To obtain a more accurate image, the sample is impregnated with an epoxy resin and is repolished using a low force. Although some pull-out is still unavoidable, most of the large porosities are no longer observed in the resulting composition of micrographs (Fig. 3(b)) or the micrograph of the central part of the image (Fig. 3(b1)). Still, smaller voids can be observed in the meat over almost the complete width of the sample. Furthermore, it is shown that the increase in fuel plate thickness has to be attributed to an increase in the thickness of the fuel meat, as the cladding shows only minor corrosion at all positions on the sample.

A detailed OM micrograph (Fig. 4) not only reveals the cellular structure of the U(Mo) agglomerate but also shows fission gas related bubbles at the U(Mo) cell boundaries.

From the secondary electron image (Fig. 5(a)) of fuel particles submitted to a lower heat flux, the thickness of

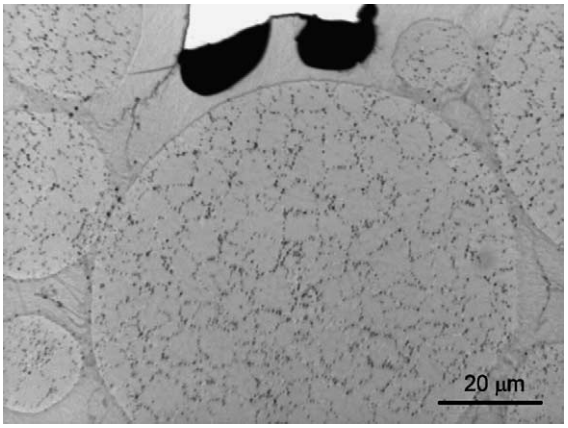

Fig. 4. Optical micrograph (as-polished condition) of a U(Mo) particle after irradiation. Fission gas related bubbles can be observed at the U(Mo) cell boundaries.

the interaction layer is measured to be approximately 4 μm. In the meat submitted to a high heat flux (central area of the sample), areas are observed where the consumption of the aluminum matrix has been completed (Fig. 5(b)). The thickness of the interaction layer at this position has increased to ≈11 μm. Although little to none of the Al matrix is left, a strong delineation of the former boundary of the U–Mo–Al interaction layer of each individual particle is present. Furthermore, it appears that the edges of the U(Mo) particles are not smooth and some of the fuel particles seem to coalesce.

The X-ray map of MoLα (Fig. 6) illustrates that the two-phase structure of the U(Mo) particle consists of U(Mo) cells surrounded by a boundary which has a lower Mo content. This is reflected in the semi-quantitative linescan (Fig. 7), where the Mo signal inside a U(Mo) agglomerate fluctuates between 6.3 and 9.0 wt%.

The Xe and Nd X-ray maps and semi-quantitative linescans (Figs. 6 and 7) show the homogeneous distribution of fission products inside the U(Mo) fuel particle. Their concentrations are lower in the U–Mo–Al reaction layer but at the interface with the Al matrix (and cladding), a clear rise in fission product concentration is observed, producing a halo around each U–Mo–Al coated fuel particle. Fig. 8 represents a linescan at a position in the fuel meat where the aluminum matrix has been completely consumed. In this case, an accumulation of fission products is observed at the position where the interaction layers of two fuel particles meet.

3.3. Composition of U–Mo–Al interaction layers

At several positions on the sample (e.g. from Fig. 8) the composition of the interaction layer has been measured. It is observed from the results summarized in Table 2, that there are two types of layers found, i.e. layers containing approximately 77 or 82 at.% Al. As the ratio of U over Mo in both phases is nearly equal to the ratio U/Mo in the original U–7wt%Mo alloy, the composition of the interaction layers can be denoted as, respectively $(U,Mo)Al_3$ and $(U,Mo)Al_{4.4}$ [9].

Table 2 also gives the amount of U, Mo and Al in the major interaction layers formed in a U–10wt%Mo vs. Al diffusion couples annealed 40 h at a temperature of 550 °C [10]. The intermediate layers L1 and L2 are approximately similar to $(U,Mo)Al_3$ and $(U,Mo)Al_{4.4}$, respectively and compare well to the composition of the interaction layers found in the current study (Fig. 9).

The third interaction layer L3 found in the out-of-pile experiment has been characterized as being very thin and high in Al and can be related to a $(U,Mo)Al_7$ layer [11], although the ratio of Mo/U in L3 is higher than in the original U(Mo) alloy. A similar phase has been found in the IRIS 1 experiment [3]. The irradiation of U–7wt%Mo ground powders at the OSIRIS

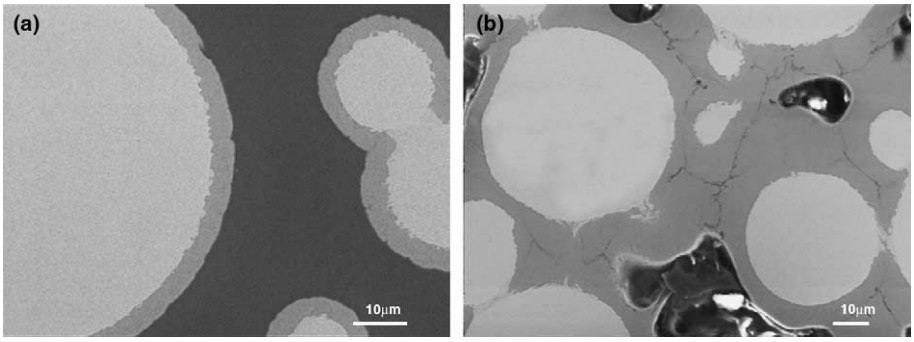

Fig. 5. The secondary electron image at a lower heat flux position (a) shows U(Mo) particles with a jagged edge surrounded by an interaction layer, dispersed in the Al matrix. The SE image of the fuel in the deformed area of the sample (b) reveals U(Mo) particles framed by a thick interaction layer. At this position the Al matrix has been completely consumed and voids appear in-between the fuel particles.

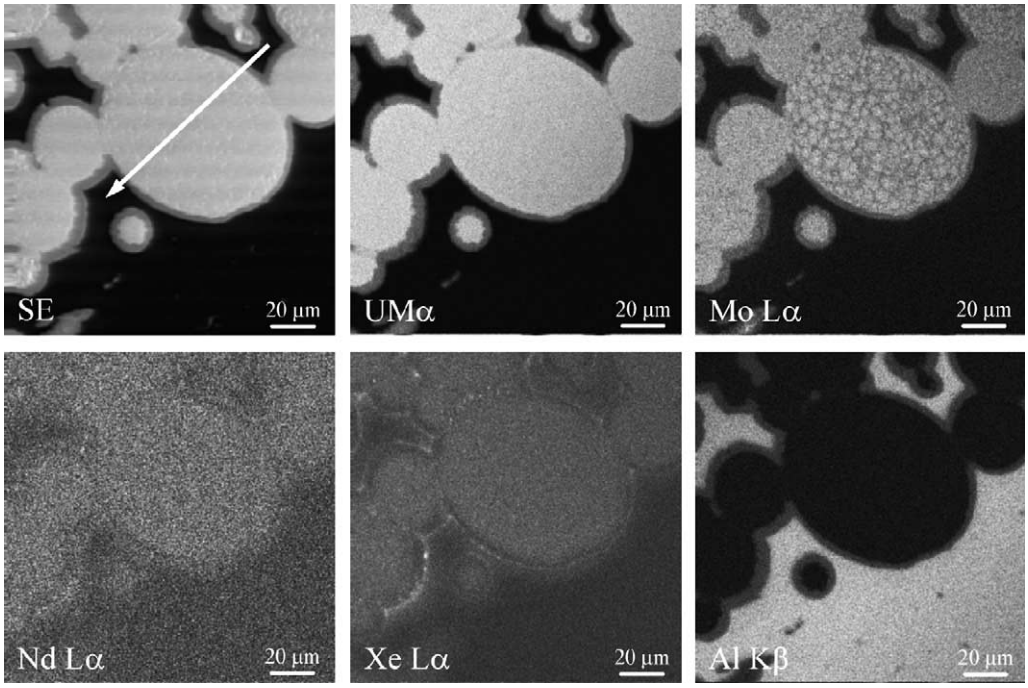

Fig. 6. Local X-ray maps of, respectively, UMα, MoLα, NdLα, XeLα and AlKα of U(Mo) particles dispersed in the Al matrix. The secondary electron image (SE) indicates the position at which a semi-quantitative linescan is measured.

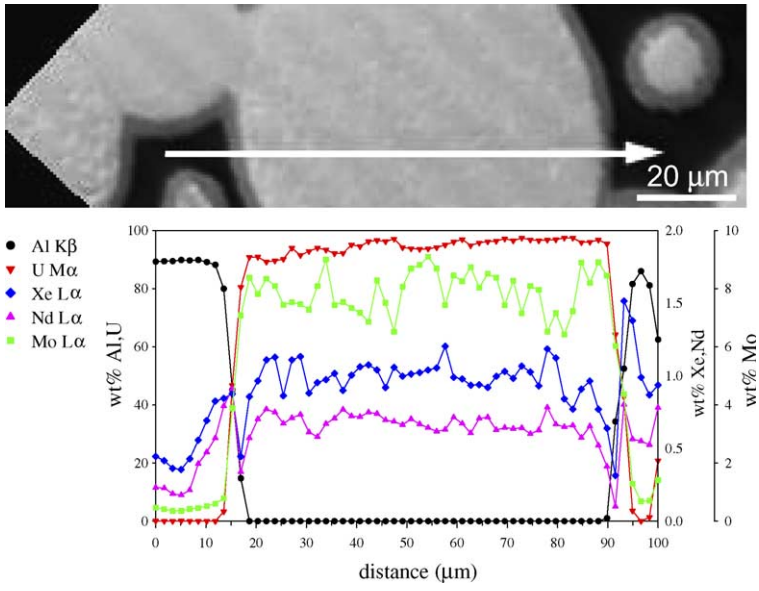

Fig. 7. Semi-quantitative X-ray analysis covering the Al matrix, the interaction layer and the U(Mo) fuel particle.

reactor resulted in the formation of interaction layers with a composition ranging between (U,Mo)Al_6 and (U,Mo)Al_8, with a Mo/U ratio nearly equal to the initial content.

3.4. MAIA code calculations

CEA has developed MAIA, a thermo-mechanical code for modeling of the U(Mo) fuel, in close collabora-

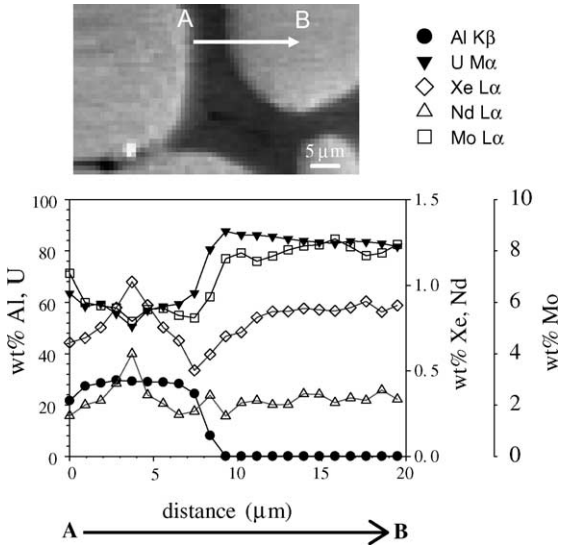

Fig. 8. Semi-quantitative X-ray analysis covering the interaction layers and part of a fuel particle. The accumulation of the fission products is seen at the junction of the interaction layers.

Table 2
Measured composition of the U–Mo–Al interaction layer (converted to at.% and normalized) at several position on the sample

	at.% Al	at.% Mo	at.% U	$\frac{\text{at.\% Al}}{\text{at.\% U+at.\% Mo}}$
	76.7	4.6	18.7	3.3
	77.2	4.0	18.8	3.4
	81.2	3.3	15.5	4.3
	82.5	3.0	14.5	4.7
	78.5	4.0	17.5	3.6
L1	77.6	4.7	17.7	3.5
L2	81.6	3.8	14.6	4.4
L3	88.3	6.3	5.4	7.6

For reasons of comparison, the composition of the interaction layers L1, L2 and L3 found in an out-of-pile study [10] are given.

tion with the Argonne National Laboratory (ANL) [3]. The code uses a finite element method for modeling of thermal and mechanical phenomena. The physical models for interaction layer growth and fission product induced swelling are the ones used in the ANL code plate lifetime accurate thermal evaluation (PLATE) [12].

Currently, the fuel swelling calculation in the MAIA code is only based on physical phenomena such as the reaction of the U(Mo) with the Al matrix with the formation of an interaction layer, fission product swelling of U(Mo), fission product swelling of the interaction layer and densification of the meat. The latter phenomenon is assumed to balance the swelling, in other words global swelling will only start if the initial porosity has totally disappeared. As the initial porosity of atomized

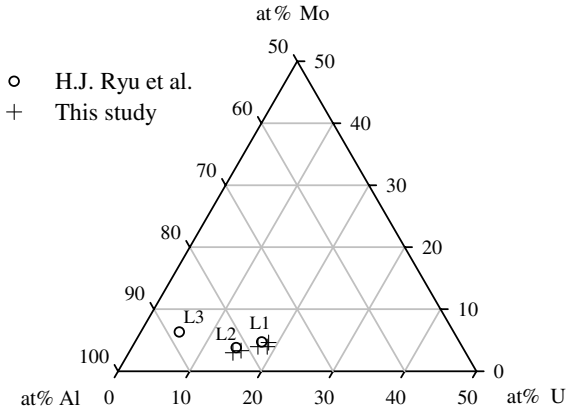

Fig. 9. The partial ternary U–Mo–Al phase diagram shows that the observed composition of the interaction layers in this study, identified as being either (U,Mo)Al3 or (U,Mo)Al4.4, are similar to the major layers (L1 and L2) found in an out-of-pile diffusion experiment [10].

fuel is very low in this case (approximately 1.1%), swelling of the fuel will start soon after the beginning of the irradiation program.

The influences of creation of voids in the fuel plate are not yet incorporated in the modeling code. Furthermore, it should be noted that MAIA is not qualified yet, and any values obtained from the code should be treated as indicative numbers and not as absolute values. Results of the MAIA calculations for the irradiation discussed in this paper are shown in Table 3.

In the current study, the volumetric evolution of the fuel particles is examined by careful image processing of the secondary electron macrographs, which give a clear contrast between the U(Mo) particle and the interaction layer. The Schwartz–Saltykov diameter analysis [13] is used to obtain the mean 3D diameter of the particles. For the fuel particles of the sibling unirradiated sample, the mean diameter is found to be 18 μm. In the irradiated sample the mean U–7wt%Mo particle diameter equals 15 μm, while the mean diameter of the fuel particle including its interaction layer equals 23 μm. The resulting volume fractions occupied by the U(Mo) fuel particles, U–Mo–Al interaction layer and Al matrix are summarized in Table 3.

4. Discussion

The optical microscopy images of the as-polished unirradiated sample and the micrographs of the irradiated sample in etched conditions show the two-phase cellular structure of the fuel particles resulting from rapid solidification during the atomization process. It is found in the literature, that the interior of each cell is molybdenum rich relative to the cell boundary. The

Table 3
The volume fraction observed in the as-fabricated and after irradiation of the U(Mo) particles, the interaction layer and the Al matrix

	U(Mo) particle (vol.%)	Interaction layer (vol.%)	Al matrix (vol.%)	Thickness interaction layer (μm)	Meat thickness increase (%)
As-fabricated					
	53	–	46	–	–
PIE					
	24	71	5	11	13
MAIA					
$(U,Mo)Al_3$	32	58	10	11.1	15
$(U,Mo)Al_{4.4}$	34	62	4	11.5	13.5
$(U,Mo)Al_7$	42	58	0	9	8

The second part of the table gives the indicative values obtained by the MAIA modeling code. The influence of a different interaction layer composition on the microstructural parameters is given.

compositional difference between the Mo enriched region in the cell interior and the Mo depleted cell boundary is approximately 2 wt% [6–8]. This is in agreement with the EPMA results, for which the X-ray mappings show a Mo depletion at the cell boundaries and the line-scan data show a fluctuation of the Mo concentration between 6.3 and 9.0 wt% inside a U(Mo) particle. The mean measured quantity for Mo of 7.9 wt% is consistent with the original added amount of Mo (7.3 wt%) increased by the amount of Mo generated during the irradiation (≈1 wt%). Because the width of the analysis area (≈1 μm) is slightly larger than the width of the cell boundary (<1 μm) it is not possible to obtain a more quantitative result on the composition of the boundary.

The X-ray diffraction pattern of the unirradiated sample reveals the existence of α-U next to the desired γ-U phase. As molybdenum is the γ-stabilizing component, it is believed that the Mo rich fuel cells consist of the stabilized γ-U, while the Mo depleted cell boundary contains more α-U. It would be at these boundaries that the interdiffusion of Al and the U(Mo) particle preferentially occurs, as the reaction of Al with γ-U is slower than with α-U [14]. In the current study the boundaries of the cells could therefore act as such diffusion pathways. The subsequent growth of an interaction layer at these cell boundaries can give the U(Mo) fuel particle edge the jagged form as observed in the SEM images.

The composition of the interaction layers ($(U,Mo)Al_3$ and $(U,Mo)Al_{4.4}$) can probably also be related to the α-uranium containing cell boundaries acting as easy diffusion pathways in the atomized U(Mo) powder. The ground powder used in the IRIS project consists of nearly pure γ-stabilized U(Mo), making the diffusion between Al and U(Mo) more difficult. However, the observed difference in interaction layer composition could also simply be the result of the lower heat flux and cladding temperature (respectively, 136 W/cm^2 and 75 °C) reached in the IRIS program opposed to the values generated in the FUTURE irradiation (respectively, 353 W/cm^2 and 130 °C).

Over almost the complete width of the sample, small voids occurring in-between the fuel meat particles are found. The origin of these voids may be found in the unidirectional Al diffusion, which can cause the creation of small voids as a result of vacancy movement which accompanies the unequal mass flow [15,16]. Similar voids have been observed in irradiated U_3Si_2 plates [17].

It is shown that the large porosities in the central area of the sample observed after the first polishing are the result of mechanical pull-out during sample preparation. Probably due to the stress zone caused by the growth of the interaction layer [18] and/or the presence of fission products at the interaction layer front, weakening of the particle boundary has occurred. Simple mechanical polishing would be enough to remove loose particles or Al matrix from the sample.

The observed swelling of the U(Mo) fuel plate has to be attributed to an increase in the thickness of the fuel meat, as the cladding shows only minor corrosion at all positions on the sample. The maximum thickness of the oxide layer on the outer surface of the fuel plate amounts to 27 μm and is located at the most deformed area.

The fission products are homogeneously dispersed in the fuel particle interior, except at the cell boundaries where fission gas bubbles can be detected. The observed halo in the X-ray maps around the fuel particles is the result of sweeping of the recoil implanted fission products by the formation and growth of the U–Mo–Al interaction layer. Consequently, the fission products accumulate at the interface of the interaction layer and the matrix and as such produce a halo around the fuel particles.

Considering the latter observation of accumulation of fission products at the U–Mo–Al coated particle periphery and the measured quantity of fission products still in the U–Mo–Al interaction layer, it is believed that, in the current case, the contribution of fission products to the overall swelling is minor. The observed increase in thickness is most probably due to the combined effect

of interaction layer formation and thermo-mechanical stresses, weakening the fuel meat cohesion and as such causing the observed pillowing.

The MAIA code calculation of some fuel parameters using different compositions for the interaction layer, is compared to the current PIE observations (Table 3). It should be noted again that the MAIA code is not fully qualified yet and does not incorporate the influence of parameters like thermo-mechanical stress or diffusion. The volume fraction of U(Mo), the U–Mo–Al interaction layer and the Al matrix after irradiation (based on the measurement of the diameters) and the thickness of the interaction layer observed in the PIE compare well to the indicative values obtained from the MAIA code.

Although the value of the fuel swelling observed in the PIE seems to be in agreement with the MAIA results, calculations on fuel swelling outside the deformed area also amount to 13% while PIE observations show a minimum swelling of the fuel plate outside the hot-spot area.

5. Conclusion

The irradiation of atomized uranium–7 wt% molybdenum fuel with a surface heat flux of maximum 353 W/cm^{2}and maximum surface cladding temperature of 130 °C resulted in a local increase of the fuel plate thickness of nearly 13% after 40 full power days.

From the post-irradiation examination it has become clear that the apparent swelling is a result of an increase in fuel meat thickness, as the cladding only shows minor corrosion. Assuming that the contribution of fission products on the fuel swelling is negligible, it is believed that the local thickness increase of 13% is the combined result of the formation of an U–Mo–Al interaction layer and the subsequent weakening of the cohesion of the meat, in combination with thermo-mechanical stresses in the fuel plate.

References

[1] S.C. Parida, S. Dash, Z. Singh, R. Prasad, V. Venugopal, J. Phys. Chem. Solids (2001) 585.
[2] G. Beghi, European Atomic Energy Community – Euratom, Report EUR 4053e, 1968.
[3] F. Huet, V. Marelle, J. Noirot, P. Sacristan, P. Lemoine, in: Proceedings of the 25th International Meeting on Reduced Enrichment for Research and Test Reactors (RERTR), Chicago, Illinois, 2003, available through the Argonne National Laboratory (ANL) website.
[4] J.M. Hamy, F. Huet, B. Guigon, P. Lemoine, C. Jarousse, M. Boyard, J.L. Emin, in: Proceedings of the 25th International Meeting on Reduced Enrichment for Research and Test Reactors (RERTR), Chicago, Illinois, 2003, available through the Argonne National Laboratory (ANL) website.
[5] G.F. Vander Voort, in: Metallography, principles and practice, ASM International, Ohio, 1999, p. 675.
[6] K.H. Kim, D.B. Lee, C.K. Kim, G.L. Hofman, K.W. Paik, J. Nucl. Mater. 245 (1997) 179.
[7] B.-S. Seong, C.-H. Lee, J.-S. Lee, H.-S. Shim, J.-H. Lee, K.H. Kim, C.K. Kim, V. Em, J. Nucl. Mater. 277 (2000) 274.
[8] K.H. Kim, J.M. Park, C.K. Kim, G.L. Hofman, M.K. Meyer, Nucl. Eng. Des. 211 (2002) 229.
[9] M.I. Mirandou, S.N. Balart, M. Ortiz, M.S. Granovsky, in: Proceedings of the 25th International Meeting on Reduced Enrichment for Research and Test Reactors (RERTR), Chicago, Illinois, 2003, available through the Argonne National Laboratory (ANL) website.
[10] H.J. Ryu, Y.S. Han, J.M. Park, S.D. Park, C.K. Kim, J. Nucl. Mater. 321 (2003) 210.
[11] G.L. Hofman, Y.S. Kim, M.R. Finlay, J.L. Snelgrove, S.L. Hayes, M.K. Meyer, C.R. Clark, in: Proceedings of the 25th International Meeting on Reduced Enrichment for Research and Test Reactors (RERTR), Chicago, Illinois, 2003, available through the Argonne National Laboratory (ANL) website.
[12] S.L. Hayes, G.L. Hofman, M.K. Meyer, J. Rest, J.L. Snelgrove, in: Proceedings of the 24th International Meeting on Reduced Enrichment for Research and Test Reactors (RERTR), San Carlos de Bariloche, Argentina, 2002, available through the Argonne National Laboratory (ANL) website.
[13] E. Underwood, in: M. Cohen (Ed.), Quantitative stereology, Addison-Wesley Publishing Company, Massachusetts, 1970, p. 119.
[14] D.B. Lee, K.H. Kim, C.K. Kim, J. Nucl. Mater. 250 (1997) 79.
[15] R.E. Reed-Hill, R. Abbaschian, in: Physical metallurgy principles, PWS, Boston, 1994, p. 360.
[16] S. Nazaré, J. Nucl. Mater. 124 (1984) 14.
[17] A. Leenaers, S. Van den Berghe, E. Koonen, P. Jacquet, C. Jarousse, B. Guigon, A. Ballagny, L. Sannen, J. Nucl. Mater. 327 (2004) 121.
[18] J.-M. Park, K.-H. Kim, D.-S. Sohn, C.-K. Kim, G.L. Hofman, J. Nucl. Mater. 265 (1999) 38.